

Dielectric-loaded surface plasmon polariton waveguides on a finite-width metal strip

J. Grandidier, G. Colas des Francs, L. Markey, A. Bouhelier, S. Massenot et al.

Citation: *Appl. Phys. Lett.* **96**, 063105 (2010); doi: 10.1063/1.3300839

View online: <http://dx.doi.org/10.1063/1.3300839>

View Table of Contents: <http://apl.aip.org/resource/1/APPLAB/v96/i6>

Published by the [American Institute of Physics](#).

Additional information on *Appl. Phys. Lett.*

Journal Homepage: <http://apl.aip.org/>

Journal Information: http://apl.aip.org/about/about_the_journal

Top downloads: http://apl.aip.org/features/most_downloaded

Information for Authors: <http://apl.aip.org/authors>

ADVERTISEMENT

**AIP**Advances

Submit Now

**Explore AIP's new
open-access journal**

- **Article-level metrics
now available**
- **Join the conversation!
Rate & comment on articles**

Dielectric-loaded surface plasmon polariton waveguides on a finite-width metal strip

J. Grandidier,^{a)} G. Colas des Francs, L. Markey, A. Bouhelier, S. Massenet, J.-C. Weeber, and A. Dereux

Laboratoire Interdisciplinaire Carnot de Bourgogne, UMR 5209 CNRS-Université de Bourgogne, 9 Av. A. Savary, BP 47 870, 21078 Dijon, France

(Received 17 December 2009; accepted 5 January 2010; published online 10 February 2010)

We investigate the guiding properties of a dielectric-loaded surface plasmon polariton waveguide on a finite-width metal strip. The guided mode is characterized by leakage radiation microscopy for different metal strip widths. We show a strong mode attenuation for metal strip widths below $1.75 \mu\text{m}$ at telecom wavelength $\lambda=1.55 \mu\text{m}$. We estimate the minimal width using numerical methods and propose an original interpretation. Good agreement with the measured data is achieved. The determination of this critical width is a prerequisite for designing miniaturized plasmonics devices. © 2010 American Institute of Physics. [doi:10.1063/1.3300839]

During the past years, there has been an increasing effort for the realization of plasmon-based components integrated on a substrate. Such devices present a high bandwidth and can overcome data transfer limitation currently existing in electronic circuitry. Surface plasmon polaritons (SPP) result from the electromagnetic wave coupling to surface density of charges. Therefore, these modes are naturally confined near the metal surface and are an alternative to standard electro-optical circuitry. Various plasmonic waveguide configurations have been investigated in the past decade: metallic nanorod,^{1,2} strip,^{3,4} slit,⁵ V-grooves,⁶ and hybrid plasmonic waveguides.⁷ Among them, the dielectric loaded surface plasmon polariton waveguide (DLSPPW) consists of a rectangular dielectric strip deposited on a metallic film.⁸ The dielectric strip induces lateral confinement of the guided mode, in addition to the intrinsic subwavelength vertical confinement of the SPP. Depending on the dielectric material properties, various functionalities are expected.^{9–11} Moreover, this simple configuration can be easily fabricated using lithography techniques so that it is a benchmark for studying plasmonic waveguide properties.

An important point concerns the integration of the polymer/metal film structure onto the surface, which requires to minimize the metal-strip width. Moreover, since the metallic strip can support both electrical and plasmonics signals, it is highly desirable to determine the widths of the metal strip compatible with plasmon waveguiding as well as electrodes using DLSPPW on finite metal strips have been numerically studied recently.¹² It was shown that the metallic strip should be larger than $3 \mu\text{m}$ to support a guided mode at telecom wavelength. This behavior clearly indicates that DLSPPW modes result from the confinement of metal/air SPP that imposes a lower limit for the width of the metal strip.^{3,13} In this letter, we experimentally investigate this effect using leakage radiation microscopy (LRM) (Ref. 10) and propose a simple and original interpretation.

The considered configuration is schematically represented in Fig. 1(a). The polymethylmethacrylate (PMMA) strip parameters were chosen since they correspond to the optimized waveguide parameters for monomodal conditions

with a good mode confinement factor.^{10,15} The gold film thickness ensures efficient characterization by leakage radiation microscopy.

The samples are fabricated using a two-level UV-lithography process with a Süss Microtech MJB4 mask aligner in the vacuum contact mode. First, we realized 50 nm thick gold strips of width w_3 varying from 1 to $3.75 \mu\text{m}$. In the second lithography level, a wavelength of 250 nm is used to fabricate the $600 \text{ nm} \times 600 \text{ nm}$ PMMA strip onto each gold strip. This step is critical and requires high precision as the 600 nm large DLSPPW must be centered on a, e.g., $1 \mu\text{m}$, metal strip. Figures 1(b)–1(d) show scanning electron micrograph (SEM) images of the obtained structures. All the PMMA strips have a width of $600 \pm 20 \text{ nm}$. They are centered onto the gold strips with an accuracy better than 60 nm . The polymer strips height is $t=600 \text{ nm}$, as checked using atomic force microscopy.

These DLSPPWs are then optically characterized by leakage radiation microscopy.¹⁰ A transverse-magnetic (TM)-polarized infrared laser beam is focused on the tapered region ($\lambda=1.55 \mu\text{m}$). Figure 2 shows the intensity recorded in the Fourier and image planes. In the Fourier plane [Fig. 2(a)], the two arcs of circles at propagation constants $\beta \approx k_0$ (effective index $n_{\text{eff}}=\beta/k_0=1$) and $\beta=1.46k_0$ ($n_{\text{eff}}=1.46$) correspond to the gold/air SPP and the planar mode TM_0 supported in the large PMMA region, respectively. The horizontal line at effective index $n_{\text{eff}}=1.27 \pm 0.01$ reveals a mode guided along the waveguide.¹⁰ This mode propagation

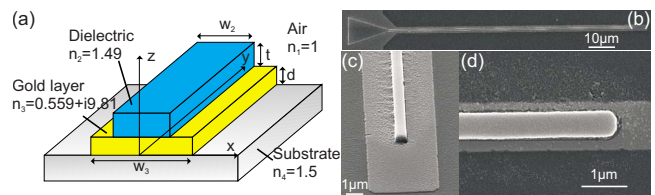


FIG. 1. (Color online) DLSPPW configuration with the corresponding notations. The polymer ridge ($t=w_2=600 \text{ nm}$) lies on a metallic strip (thickness $d=50 \text{ nm}$) atop a glass substrate. Refractive indices are given at $\lambda=1.55 \mu\text{m}$ (Ref. 14). [(b)–(d)] SEM of the studied DLSPPWs [(b): large view including the excitation taper, [(c) and (d)]: PMMA strip centered onto a $3.75 \mu\text{m}$ (c) or $1.00 \mu\text{m}$ (d) metallic strip].

^{a)}Electronic mail: jonathan.grandidier@u-bourgogne.fr.

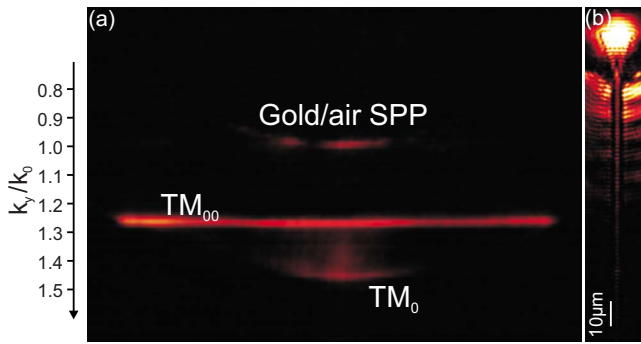


FIG. 2. (Color online) LRM observation of the propagation along the waveguide in the (a) Fourier plane and in the (b) image plane. In (b), the gold/SPP mode and the TM_0 mode are used to calibrate the Fourier plane. The gold strip width is $w_3=3.50 \mu\text{m}$.

is also visible in the image plane, with a characteristic propagation length $L_{\text{SPP}}=19.5 \pm 2 \mu\text{m}$. We have repeated these measurement for all gold strips widths.

Figure 3(a) presents the mode propagation length as a function of the metal width. We also plot the calculated values obtained using either the differential¹² or Green's dyad method,¹⁶ demonstrating a rather good agreement between measured and calculated propagation lengths. A critical gold strips width appears at $w_3^{\text{min}}=1.75 \mu\text{m}$. This critical value is lower than the value calculated in Ref. 12. This difference is only due to the different gold dielectric constant used here.¹⁴ Below w_3^{min} , the propagation length dramatically drops. The mode profiles are represented on Figs. 3(b) and 3(c). In case of a narrow gold strip, the guided mode strongly interacts with the metallic strip corners and strong losses also clearly appear into the substrate. We discuss hereafter the origin of

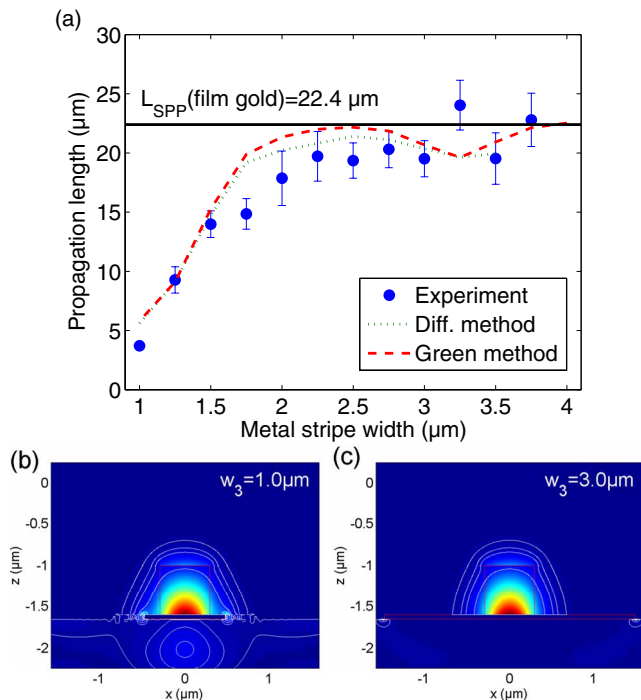


FIG. 3. (Color online) (a) Propagation length of the guided mode for different metal strip widths. The measured values and numerical simulation using differential method and Green method are represented. Effective index model leads to a constant propagation length $21.8 \pm 0.1 \mu\text{m}$ (not shown). [(b) and (c)] The mode intensity profiles are presented for a narrow (b) and large gold strip (c).

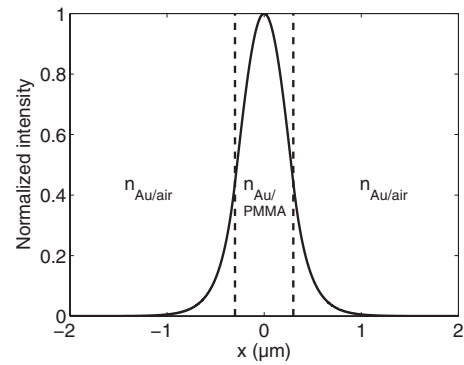


FIG. 4. Mode intensity profile obtained applying the effective index model to a $600 \text{ nm} \times 600 \text{ nm}$ PMMA strip on a infinitely extended 50 nm gold film. The slab equivalent to the DLSPPW is described on the figure.

this minimal width necessary to ensure good mode propagation length.

For this purpose, we consider the effective index model, recently adapted to the DLSPPW configuration.¹⁵ Effective index model relies on a representation of the two-dimensional strip geometry to an equivalent one-dimensional (1D) slab geometry. Specifically, the $w_2 \times t$ PMMA strip on gold waveguiding structure is assimilated to a symmetric slab waveguide of width w_2 . The core index is the gold/PMMA SPP effective index $n_{\text{Au/PMMA}}$ that takes into account the dielectric thickness t ($n_{\text{Au/PMMA}}=1.449$ for $t=600 \text{ nm}$). The clad index is the gold/air effective index $n_{\text{Au/air}}$ ($n_{\text{Au/air}}=1.005$). We claim that the gold strip width should be larger than the guided mode extension to keep good propagation properties. Figure 4 represents the slab mode profile. The mode intensity is negligible (less than 1% its maximum value) outside a region of $1.8 \mu\text{m}$ in agreement with the critical value w_3^{min} observed above. The exact DLSPPW mode profile calculated on Fig. 3(b) for a $w_3=1 \mu\text{m}$ gold strip confirms that the plasmon mode strongly interacts with the gold strip corners. This interaction with the gold corners cannot be described within the 1D effective index model, so that it fails to evaluate the mode propagation length when applied to narrow gold strips. Note also that effective index approximation that considers finite gold films presents a mode effective index decrease at small widths¹³ in contradiction with the calculated one (Fig. 5). However, when it is

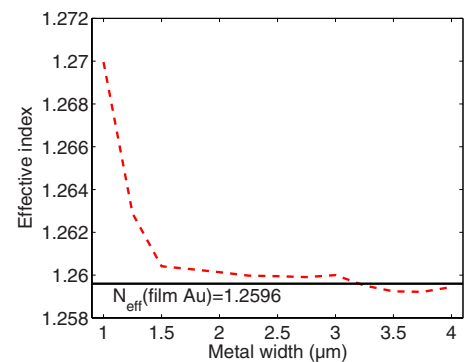


FIG. 5. (Color online) Effective index of the DLSPPW guided mode calculated using Green's dyad method, as a function of the gold strip width.

applied to a PMMA strip on an extended gold film, this quantitatively reproduces the SPP mode extension. Since no SPP mode can be supported outside the metal, this mode extension indicates the minimal metallic film size.

In addition, this plasmon mode extension imposes a supplementary condition on the dielectric strip position on the finite gold film. Indeed, the gold/air regions located on each side of the PMMA strip should also be sufficient to support the plasmon mode. To check this, we fabricated PMMA strips (500 nm height and 900 nm width) on a gold strip. In case of PMMA strip approximately centered on a large gold strip ($w_3=3.75 \mu\text{m}$), we measured $L_{\text{SPP}}=19.4 \pm 1.9 \mu\text{m}$. It drops to $L_{\text{SPP}}=15.5 \pm 0.8 \mu\text{m}$ for a PMMA strip having an edge at 550 nm from the edge of a $2.5 \mu\text{m}$ wide gold strip.

In conclusion, dielectric waveguides lying on finite metal strips have been fabricated and then numerically and experimentally characterized. We demonstrate that strong DLSPPW mode attenuation for narrow metal strips. A simple model is discussed that quantitatively estimates the minimal metal width above which the mode propagation length is maximized. The agreement between numerical simulations, measured propagation lengths and this simple model clearly demonstrate that the guided mode is a plasmon mode. Finally, we observed strong field localization at the metal edge. This phenomenon will be investigated in the very near future.

This work was financially supported by the European Commission (PLASMOCOM Project No. EC FP6 IST 034754 STREP).

- ¹R. M. Dickson and L. Lyon, *J. Phys. Chem. B* **104**, 6095 (2000).
- ²H. Ditlbacher, A. Hohenau, D. Wagner, U. Kreibig, M. Rogers, F. Hofer, F. R. Aussenegg, and J. R. Krenn, *Phys. Rev. Lett.* **95**, 257403 (2005).
- ³J.-C. Weeber, Y. Lacroute, and A. Dereux, *Phys. Rev. B* **68**, 115401 (2003).
- ⁴P. Berini, *Phys. Rev. B* **63**, 125417 (2001).
- ⁵H. T. Miyazaki and Y. Kurokawa, *Phys. Rev. Lett.* **96**, 097401 (2006).
- ⁶S. I. Bozhevolnyi, V. S. Volkov, E. Devaux, J.-Y. Laluet, and T. W. Ebbesen, *Nature (London)* **440**, 508 (2006).
- ⁷R. Oulton, V. Sorger, D. A. Genov, D. F. P. Pile, and X. Zhang, *Nat. Photonics* **2**, 496 (2008).
- ⁸B. Steinberger, A. Hohenau, H. Ditlbacher, A. L. Stepanov, A. Drezet, F. R. Aussenegg, A. Leitner, and J. R. Krenn, *Appl. Phys. Lett.* **88**, 094104 (2006).
- ⁹A. V. Krasavin and A. V. Zayats, *Phys. Rev. B* **78**, 045425 (2008).
- ¹⁰J. Grandidier, S. Massenet, G. Colas des Francs, A. Bouhelier, J.-C. Weeber, L. Markey, A. Dereux, J. Renger, M. U. González, and R. Quidant, *Phys. Rev. B* **78**, 245419 (2008).
- ¹¹J. Grandidier, G. Colas des Francs, S. Massenet, A. Bouhelier, L. Markey, J. Weeber, C. Finot, and A. Dereux, *Nano Lett.* **9**, 2935 (2009).
- ¹²S. Massenet, J.-C. Weeber, A. Bouhelier, G. Colas des Francs, J. Grandidier, L. Markey, and A. Dereux, *Opt. Express* **16**, 17599 (2008).
- ¹³R. Zia, M. S. Schuller, and M. L. Brongersma, *Phys. Rev. B* **71**, 165431 (2005).
- ¹⁴E. D. Palik, *Handbook of Optical Constants of Solids* (Academic, New York, 1998).
- ¹⁵T. Holmgaard and S. I. Bozhevolnyi, *Phys. Rev. B* **75**, 245405 (2007).
- ¹⁶G. Colas des Francs, J. Grandidier, S. Massenet, A. Bouhelier, L. Markey, J.-C. Weeber, and A. Dereux, *Phys. Rev. B* **80**, 115419 (2009).